Environ Monit Assess (2011) 172:235–247
DOI 10.1007/s10661-010-1330-x

Polycyclic aromatic hydrocarbons in the atmosphere of Shanghai, China

Yingjun Chen · Yanli Feng · Shengchun Xiong · Dongyan Liu · Gang Wang · Guoying Sheng · Jiamo Fu

Received: 19 May 2009 / Accepted: 18 January 2010 / Published online: 10 February 2010

Abstract Shanghai is the largest industrial and commercial city in China, and its air quality has been concerned for several years. However, scarce study had been made on the seasonal levels of atmospheric polycyclic aromatic hydrocarbons (PAHs), together with their gas–particle partitioning and potential emission sources. Based on an intensive sampling campaign at urban and suburban areas in Shanghai during four seasons of 2005–2006, this study presented the measurement of PAH concentrations in both particulate and gaseous phases, as well as seasonal and spatial variability. The results showed that the annual PAH levels (gas + particle) were 167 ± 109 ng m^{-3} at the urban site and 216 ± 86.5 ng m^{-3} at the suburban site. Gaseous PAHs (>70%) dominated the total PAH mass at both sites, while particulate PAHs contributed more than 90% of the toxic power according to benzo(*a*)pyrene-equivalent carcinogenic parameter. Different seasonal trend of PAH concentrations was observed between the two sites, and it may be explained by complicated factors such as sampling heights, local/regional emission sources, and climatic conditions. The gas–particle partitioning of PAHs in all samples was calculated, and strong linear correlations between log K_p and log P_L^o were observed, with shallower slopes (m_r) at the suburban site than the urban one and in warm season than the cold months, indicating the different equilibrium conditions of PAHs in spatial and seasonal scales in Shanghai. The slope ($m_r = -0.96$) and correlation coefficient ($R^2 = 0.81$) for four-ring PAHs were closest to theoretical equilibrium conditions among compounds with various aromatic rings. Finally, the potential PAH sources were estimated based on principal factor analysis with multiple linear regressions. Ground volatilization dominated the PAH pollutions at both sites, while vehicles and coal consumption were the other main emission sources, which totally contributed 32.0% (suburban) to 49.2% (urban) of PAH mass in Shanghai atmosphere. The effects of wood and biomass burning were also detected, but their contributions to PAHs were negligible.

Y. Chen · D. Liu · G. Wang
Yantai Institute of Coastal Zone Research, Chinese Academy of Sciences, Yantai, Shandong Province, 264003, China

Y. Feng (✉) · S. Xiong
Institute of Environmental Pollution and Health, School of Environmental and Chemical Engineering, Shanghai University, Shanghai, 200444, China
e-mail: fengyanli@shu.edu.cn

G. Sheng · J. Fu
State Key Laboratory of Organic Geochemistry, Guangzhou Institute of Geochemistry, Chinese Academy of Sciences, Guangzhou, 510640, China

Keywords PAHs · Concentration · Seasonal trends · Gas–particle partitioning · Source apportionment · Shanghai

Introduction

Polycyclic aromatic hydrocarbons (PAHs) are a class of ubiquitous environmental pollutants, which have drawn a great concern for several decades due to potential carcinogenic and mutagenic properties (IARC 1987). Atmospheric PAHs are important by-products of incomplete combustion or pyrolysis of fossil fuels and other organic materials such as wood and biomass. In urban areas, PAHs mainly derived from anthropogenic activities, including vehicular exhaust, industrial and domestic emissions (Ravindra et al. 2008), and the sources varied from region to region. For example, fireplace combustion of wood for residential heating is an important source of PAH compounds in many cities of the USA during winter months (Schauer et al. 2001), while various coal stoves contribute significantly to the indoor and outdoor PAH pollution in China (Chen et al. 2005). Evaporations from contaminated ground in urban areas may be an additional source of PAHs in warm seasons (Dimashki et al. 2001; Li et al. 2006).

Atmospheric PAHs usually occur in both particulate and gaseous phases, depending on the vapor pressure of each compound. Generally, low molecular weight PAHs (two to three rings) tend to be more abundant in gas phase, while higher weight ones (five or more rings) are often associated with particles. The distribution of PAHs between the phases is of scientific interest due to some reasons. Particle-bound PAH compounds usually contain large fraction of more carcinogenic homologues such as benzo(*a*)pyrene (B*a*P), while gaseous PAHs are more abundant in urban areas and can produce much more toxic derivatives through reaction with other pollutants. Furthermore, gas–particle partitioning is an important factor on the fate, transport, and removal of PAHs from the atmosphere by dry and wet deposition processes (Bidleman 1988; Offenberg and Baker 2002; Poor et al. 2004). The chemical degradation of PAHs is also influenced by the phase distribution: vapor PAHs are susceptible to transform via OH radical, while particulate ones are susceptible to photochemical reactions (Finlayson-Pitts and Pitts 2000).

Shanghai (31.1° N, 121.4° E) is the largest industrial and commercial city in China with a population over 18 million. It is located at the east end of the Yangtze River Delta and faces the East China Sea. During the past decades, Shanghai has experienced rapid development of urbanization and industrialization. Large coal consumption for power plants and industries together with soaring-up vehicular population severely deteriorated the air quality in this region (Chen 2003). Although the air quality has been improved obviously since mid-1990s, fine particles ($PM_{2.5}$) and their organic fraction remained the priority pollutant in the ambient air, and haze was observed sometimes hanging over the city during fall (Feng et al. 2009). Therefore, for the purpose of control and abatement of the organic contamination and especially the PAH proportion, it is necessary to investigate the extent of PAH pollution as well as the source apportionment in Shanghai atmosphere. Based on an intensive sampling campaign during 2005–2006 at both urban and suburban sites in Shanghai, this study focused on (1) determination of PAH concentrations and their seasonal trends, (2) characteristics of gas–particle partitioning, and (3) investigation of potential sources of PAHs.

Experimental section

Sample collection

The two sites selected for sample collection in this study included an urban site located in Zha-bei District (ZB) of downtown Shanghai and a suburban site in Jia-ding District (JD). The detailed information of these sites was presented elsewhere (Feng et al. 2009), and a brief description was given as follows. The ZB site was situated on the rooftop of a nine-storey office building (ca. 25 m in height) in the Yan-chang campus of Shanghai University and represented a mixed res-

idential/traffic/commercial environment in urban area. The JD site was located on the rooftop of a four-storey office building (ca. 10 m in height) at the Environmental Monitoring Station of Jia-ding District and represented a residential and slightly industrialized environment of suburban area. The distance of the two sites was about 30 km.

Sampling was conducted simultaneously at both sites in dry weather days in October 2005 and January, April, and July 2006. The 4 months were selected because they could stand for the four seasons from fall to summer, respectively, and the representativeness has been explained in detail previously (Feng et al. 2009). During each sampling month, eight pairs of particle–gas samples were collected using high-volume air samplers (Wuhan Tianhong Intelligent Instrument, China) at a flow rate of ~450 L min^{-1}. The actual flow was carefully calibrated before and after sampling with a flow calibrator. A Whatman glass-fiber filter (GFF, 20.3 × 25.4 cm) was used to collect total suspended particles (TSP) and a polyurethane foam (PUF) plug (length 8.0 cm by diameter 6.25 cm) to absorb vapor organic compounds. Each sampling began at 10:00 A.M. and lasted for consecutive 24 h, and the meteorological parameters were recorded at the beginning and end of sampling using a portable weather monitor (Kestrel-1000, USA), including ambient temperature, relative humidity, and wind speed/direction. Totally, 64 pairs of field GFF/PUF samples were collected at the two sites.

Prior to sampling, all GFFs were baked at 450°C for 5 h, and then wrapped in aluminum foil packages. The PUF plugs were soxhlet-extracted for 72 h in dichloromethane (DCM), dried in vacuum desiccators, and sealed in precleaned jars. After sampling, GFF and PUF samples were sealed and brought back to the laboratory. The TSP mass concentration was determined by weighing the filter before and after particle deposition using an electronic balance (Satouris LA130-F, Germany). Before weighing, each filter was conditioned under 25°C and 50% RH for 24 h in a temperature- and moisture-controlled climate chamber (Binder KBF-115, Germany). All samples were stored in a freezer at −20°C until analysis.

Analytical procedure

Sixteen PAH standards (United States Environmental Protection Agency Method 610) in a mixture were purchased from Supleco (USA). Seven deuterated PAH standards (ES-2044), including naphthalene (NAP)-d_8, acenaphthylene (ACY)-d_8, phenanthrene (PHE)-d_{10}, fluoranthene (FLO)-d_{10}, pyrene (PYR)-d_{10}, B*a*P-d_{12}, and benzo(*ghi*)perylene (B*ghi*P)-d_{12}, were obtained from Cambridge Isotope Corporation (USA). Coronene and hexamethylbenzene were acquired initially as a solid of 99% purity from Aldrich Chemical (USA). All reagents utilized were redistilled in all-glass distilling appliance.

Glass-fiber filter samples were cut into strips and extracted three times with 100-mL DCM using ultrasonic extraction, and each extraction lasted 30 min. Polyurethane foam plugs were extracted for 72 h with 250-mL DCM in a soxhlet apparatus. Deuterated PAH standards were added to all samples as surrogates prior to extraction. The extracts were filtered, combined, and concentrated on a rotary evaporator (Heidolph Laborota 4011-digital, Germany) with bath temperature ≤30°C. After transformation of the solvent into *n*-hexane, extract of each sample was fractionated through a 2:1 silica–alumina gel column, and the PAH fraction was collected by eluting the column with 100-mL *n*-hexane–DCM mixture (7:3). Then, the sample was reduced to ~0.5 mL under a gentle stream of ultrapurified nitrogen. Prior to instrumental analysis, known quantities of internal standard (hexamethylbenzene) solution were added into the samples.

All samples were analyzed with Agilent 6890 gas chromatography and 5975 mass selective detection in the electron impact mode (70 eV). An HP-5ms capillary column (30 m × 0.25 mm i.d. × 0.25 μm thickness) was used for PAH separation. The instrumental conditions were as follows: injector temperature, 300°C; ion source temperature, 180°C; injection volume, 1 μL; splitless model; carrier gas, helium with constant flow rate of 1.0 mL min^{-1}; temperature program: 65°C (3 min), 65°C to 300°C at 5°C min^{-1}, and 300°C (10 min); mass range, m/z 50 to 500. Data acquisition and processing were controlled by a Chemsta-

tion data system. Chromatographic peaks of samples were identified by authentic standards and by mass spectra. Twenty-seven PAH compounds were quantified in the samples, including 17 commonly discussed PAHs such as ACY, acenaphthene (ACE), fluorine (FLU), PHE, anthracene (ANT), FLO, PYR, benzo(*a*)ANT (B*a*A), chrysene (CHR), benzo(*b*)FLO (B*b*F), benzo(*k*)FLO (B*k*F), benzo(*e*)PYR (B*e*P), B*a*P, indeno(1,2,3-*cd*)PYR (I*cd*P), B*ghi*P, dibenzo(*a*,*h*)ANT (DBA), and coronene (COR) and 10 other compounds for source identification such as retene (RET), dibenzofuran (DBF), dibenzothiophene (DBT), acephenanthrylene (ACP), indeno(1,2,3-*cd*)FLO (I*cd*F), benzo(*ghi*)FLO (B*ghi*F), and methyl derivatives (M-) of FLU, PHE, PYR, and CHR.

Quality assurance/quality control

Eight pairs of GFF/PUF samples were collected as field blanks to determine any background contamination for the two sites in four seasons, accompanied by another two pairs of lab blanks and spiked blanks. All blank samples were analyzed together with the field samples using the same procedure.

Polycyclic aromatic hydrocarbons in the filter blank samples were below detection limit, while some lighter compounds such as PHE were determined in the PUF blanks. The average recoveries for surrogates in field samples were NAP-d_8 36%, ACY-d_8 78%, PHE-d_{10} 107%, FLO-d_{10} 116%, PYR-d_{10} 106%, B*a*P-d_{12} 105%, and B*ghi*P-d_{12} 95%. The average recoveries for 16 PAHs in the spiked blanks varied from 39% (NAP) to 122% (B*ghi*P). All PAH concentrations in the samples were corrected for recovery efficiencies, except NAP, which was excluded from the interested compounds due to low recovery in this study.

Results and discussion

Levels of TSP mass in Shanghai

The seasonal and annual values of TSP mass concentration and meteorological conditions for the samples at both the ZB and JD sites are presented in Table 1. It can be seen that the level and seasonal variation of TSP abundance between the two sites were very similar, suggesting the equivalent particulate matter (PM) pollution in suburban area to urban area of Shanghai. The annual TSP concentration was about 204 μg m^{-3}, a little higher than the Chinese TSP standard level (200 μg m^{-3}) for class II areas, which refer to most urban and rural areas (http://www.envir.gov.cn/law/airql.htm). The most serious TSP pollution occurred in spring and fall, indicating the significant influence of dust storm in spring and haze weather (usually when low level temperature inversion occurs) in fall on the air quality of Shanghai. For example, the strong dust storm on April 19–20, 2006 affected wide areas in China, and the highest TSP concentration was recorded at the urban site as 638 μg m^{-3}, two times higher than the daily TSP standard of 300 μg m^{-3} for class II areas. Summer is the cleanest season, with the TSP level lower than in spring by a factor of 2.5, mainly attributed to the clean winds coming from the East China Sea together with abundant precipitation. This seasonality of TSP concentration was similar to $PM_{2.5}$ concentrations concurrently

Table 1 Total suspended particle concentrations (avg. ± SD) and meteorological conditions for Shanghai samples

Site	Period	TSP (μg m^{-3})	Temperature (°C)	Pressure (kPa)	RH (%)	Prevailing wind
ZB	Fall	262 ± 120	22.3 ± 2.7	101.8 ± 0.4	41.2 ± 13.8	Northeast
	Winter	171 ± 66.9	9.9 ± 2.6	102.0 ± 0.4	44.8 ± 11.8	Northwest
	Spring	291 ± 161	21.8 ± 3.8	101.1 ± 0.5	37.1 ± 7.0	Southeast
	Summer	105 ± 63.3	32.0 ± 1.6	100.2 ± 0.3	63.0 ± 6.4	Southeast
	Annual	204 ± 129	21.8 ± 8.6	101.3 ± 0.8	47.5 ± 14.1	
JD	Fall	245 ± 94.8	23.0 ± 3.7	101.9 ± 0.4	42.4 ± 9.7	Northeast
	Winter	183 ± 41.4	9.3 ± 3.2	102.4 ± 0.4	48.9 ± 10.7	Northwest
	Spring	266 ± 88.1	22.1 ± 4.3	101.3 ± 0.5	43.1 ± 11.2	Southeast
	Summer	121 ± 25.4	34.1 ± 2.4	100.6 ± 0.3	57.0 ± 10.1	Southeast
	Annual	204 ± 88.4	22.5 ± 9.4	101.5 ± 0.8	47.8 ± 11.6	

measured at both sites (Feng et al. 2009). However, the severity of PM pollution in Shanghai should be more concerned when fine particle was focused because the annual $PM_{2.5}$ levels at both sites exceeded 90 μg m^{-3}, six times over the US National Ambient Air Quality Standard (15 μg m^{-3}, http://www.epa.gov/air/criteria.html).

Characteristics of total PAH concentrations

The annual average of total concentrations (gas plus particle phases) of the 17 PAHs were 167 ± 109 and 216 ± 86.5 ng m^{-3} at the ZB and JD sites, respectively (Table 2). More serious PAH pollution was observed at the suburban site than the urban one, which may be attributable to the relocation of industrial plants away from urban center in recent years as well as the influence of sampling heights. Compared with the measurements at other urban areas around the world (Table 3), atmospheric PAH level in Shanghai was lower than Taichung (789 ng m^{-3}), Chicago (423 ng m^{-3}), Guangzhou (334 ng m^{-3}), and Rome (270 ng m^{-3}) but obviously higher than other areas such as Seoul (78.1 ng m^{-3}), Prato (59.4 ng m^{-3}), Heraklion (56.6 ng m^{-3}), Fuji (45.6 ng m^{-3}), Izmir (35.4 ng m^{-3}), Shimizu (28.5 ng m^{-3}), Baltimore (24.2 ng m^{-3}), and Athens (17.6 ng m^{-3}; references listed in Table 3).

Similar PAH profiles were seen at the ZB and JD sites (Fig. 1). Phenanthrene was the most abundant compound and accounted for about 40% of total PAH mass (ΣPAHs), followed by FLO, PYR, ANT, and FLU, while other 12 PAHs totally contributed less than 25%. This result was similar to the occurrence of PAHs in Guangzhou (Li et al. 2006), where PHE predominated the total mass (~60%) and the above-mentioned five compounds totally contributed 92%, as well as many other areas around the world such as Heraklion in Greece (Tsapakis and Stephanou 2005), although the PAH level was much higher in Shanghai.

The dependence of gas–particle partitioning of individual PAH on its aromatic ring number was consistent with other studies (Bi et al. 2003; Cincinelli et al. 2007), i.e., three-ring PAHs (ACY, ACE, FLO, PHE, and ANT) primarily existed in the vapor phase (>90%), while five- or more ring PAHs were mainly associated with the particles (Fig. 1). The particulate PAHs contributed less than 30% of total PAH mass but accounted for

Table 2 Annual concentrations (avg. ± SD) of total PAHs (gas + particle) and the particulate fraction in Shanghai samples

PAH compounds	Abbr.	ZB site		JD site	
		Concentration (ng m^{-3})	Particle (%)	Concentration (ng m^{-3})	Particle (%)
Acenaphthylene	ACY	0.79 ± 0.83	0 ± 0	1.33 ± 2.32	0 ± 0
Acenaphthene	ACE	0.56 ± 0.37	0 ± 0	0.74 ± 1.16	0 ± 0
Fluoranthene	FLU	8.89 ± 8.01	1.70 ± 2.60	8.37 ± 5.77	1.70 ± 3.20
Phenanthrene	PHE	67.6 ± 42.1	2.10 ± 2.20	79.5 ± 37.2	1.50 ± 1.30
Anthracene	ANT	9.80 ± 7.20	9.2 ± 12.7	11.7 ± 7.04	10.1 ± 9.5
Fluoranthene	FLO	23.5 ± 17.5	13.8 ± 10.8	36.8 ± 27.5	10.9 ± 9.3
Pyrene	PYR	14.3 ± 10.2	17.1 ± 12.0	23.6 ± 16.2	13.5 ± 11.5
Benz(*a*)anthracene	B*a*A	3.10 ± 2.96	66.6 ± 29.5	4.84 ± 2.25	65.5 ± 29.2
Chrysene	CHR	5.87 ± 5.50	70.2 ± 19.9	7.41 ± 3.27	64.7 ± 25.5
Benzo(*b*)fluoranthene	B*b*F	6.58 ± 5.14	94.3 ± 8.00	7.84 ± 3.91	85.5 ± 27.2
Benzo(*k*)fluoranthene	B*k*F	3.89 ± 3.37	94.7 ± 18.4	5.13 ± 3.01	80.6 ± 37.0
Benzo(*e*)pyrene	B*e*P	4.21 ± 3.19	97.1 ± 5.70	5.55 ± 2.77	88.9 ± 25.4
Benzo(*a*)pyrene	B*a*P	2.63 ± 2.84	98.2 ± 3.70	3.15 ± 2.67	97.8 ± 3.40
Indeno(1,2,3-*cd*)pyrene	INP	6.02 ± 6.95	100 ± 0	8.16 ± 5.44	100 ± 0
Dibenzo(*a*,*h*)anthracene	DBA	2.86 ± 2.92	100 ± 0	4.07 ± 3.11	100 ± 0
Benzo(*ghi*)perylene	B*ghi*P	2.60 ± 3.85	100 ± 0	3.60 ± 3.41	100 ± 0
Coronene	COR	3.65 ± 3.31	100 ± 0	4.32 ± 3.17	100 ± 0
ΣPAHs		167 ± 109	26.4 ± 14.9	216 ± 86.5	27.5 ± 15.5
B*a*P-equivalent carcinogenic power	B*a*PE	5.75 ± 5.71	95.6 ± 10.2	7.44 ± 5.26	89.0 ± 22.6

Table 3 Total PAH concentrations (gas + particle, ng m^{-3}) measured at urban and suburban areas around the world

City/Country	PAH level	Site	Period	PAHs summed	Reference
Shanghai/China	167	Urban	Annual	17 (listed in Table 2)	This study
	216	Suburban	Annual	17	
Guangzhou/China	124	Urban	Spring–summer	17	Bi et al. (2003)
	334	Urban	Annual	15, missed BeP and COR	Li et al. (2006)
Taichung/Taiwan	789	Urban	Summer–winter	17	Fang et al. (2004)
Chicago/USA	423	Urban	Summer–fall	13, missed ACY, BeP, DBA and COR	Odabasi et al. (1999)
Rome/Italy	270	Urban	Annual	17	Possanzini et al. (2004)
Seoul/Korea	78.1	Urban	Annual	15, missed BeP and COR	Park et al. (2002)
Fuji/Japan	45.6	Urban	Summer–winter	16, missed ACY	Ohura et al. (2004)
Shimizu/Japan	28.5	Urban	Summer–winter	16, missed ACY	
Baltimore/USA	24.2	Urban	Summer	15, missed ACY and ACE	Dachs et al. (2002)
Athens/Greece	17.6	Urban	Summer	15, missed ACY and ACE	Mandalakis et al. (2002)
	28.2	Suburban	Summer–winter	14, missed ACY, ACE and COR	Vasilakos et al. (2007)
Heraklion/Greece	56.6	Urban	Annual	15, missed ACY and ACE	Tsapakis and Stephanou (2005)
Prato/Italy	59.4	Urban	Mar.–Nov.	14, missed ACY, ACE and FLU	Cincinelli et al. (2007)
Izmir/Turkey	35.4	Urban	Summer–winter	14, missed ACY, BeP and COR	Bozlaker et al. (2008)

more than 90% of total toxic power. For example, other than the sole B*a*P (98% existed on particles), another parameter for PAH carcinogenicity expression, namely, B*a*P-equivalent carcinogenic power (B*a*PE) that was introduced by Cecinato (1997), was calculated as 5.75 and 7.44 ng m^{-3} at the ZB and JD sites, respectively, of which 89–96% derived from the particle phase (Table 2).

Seasonal variations of PAH concentrations

Seasonal trends of PAH abundance were different between the two sites (Fig. 2). The total PAH concentration at the ZB site decreased gradually from fall (256 ng m^{-3}) to summer (113 ng m^{-3}), and the variation ratio was 2.3, while at the JD, it increased from winter (178 ng m^{-3}) to summer

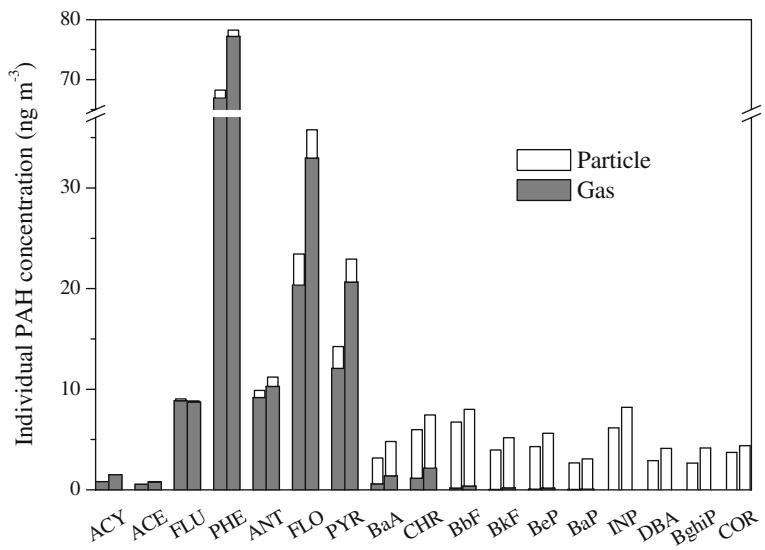

Fig. 1 Annually averaged PAH profiles at the ZB (left) and JD (right) sites in Shanghai

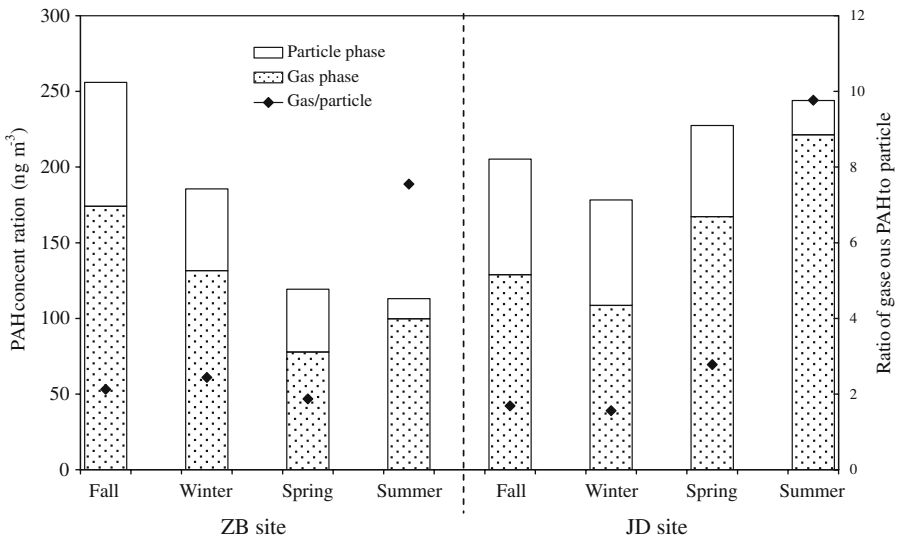

Fig. 2 Seasonal trends of total PAH concentrations and their gas-to-particle ratios at the ZB and JD sites

(244 ng m^{-3}) with the variation ratio of 1.4. From the other side, PAH levels in spring and summer were obviously lower among the four seasons at the ZB site but relatively higher at the JD, and the corresponding values differed by two times between the two sites, compared with the 20% difference in fall and almost equivalent levels in summer (Fig. 2). These seasonal characteristics may be attributable to complicated factors, including the heights of the sampling sites, local/regional emission sources, and climatic conditions such as haze weather that occurred more frequently in fall at the urban site. For example, the ZB site stood the highest location around (ca. 25 m above the ground) and was affected by regional emission sources to a larger extent, compared with the JD site that had no predominance around in height (ca. 10 m) and might be easily affected by local sources such as small chimneys from a glass factory nearby (Feng et al. 2009). The evaporation of PAHs from contaminated ground during warm months was an additional reason for the different PAH levels between the urban and suburban sites (Li et al. 2006). Liu et al. (2007) recently reported an obviously spatial distribution of PAH concentration in road dust among various functional areas in Shanghai.

The distribution of PAHs between the gas and particle phases varied with the seasons at the two sites, as shown in Fig. 2. The gaseous PAH concentration at the ZB site varied from 77.8 ng m^{-3} in spring to 174 ng m^{-3} in fall, while it was in the range of 109 ng m^{-3} in winter to 221 ng m^{-3} in summer at the JD site. The ratio of gas- to particle-phase PAH abundances was the highest in summer (7.5 for the ZB site and 9.8 for the JD) and obviously higher than the value in other seasons. This may be simply explained by the effect of ambient temperature. However, the weak fluctuation of the ratios of gas–particle PAHs among the other three seasons may derive from the seasonal shift of emission sources in Shanghai.

Different from the total PAH levels, carcinogenic parameters (B*a*P and B*a*PE) showed consistent seasonal variation between the two sites: fall > spring > winter > summer, and the ratios of fall to summer for both parameters were about 5 at the ZB site while about 3 at the JD site, indicating the most serious PAH pollution in fall. This is true when comparing the B*a*P concentrations with the daily B*a*P level in Chinese ambient air quality standard (10 ng m^{-3}), i.e., there were two days in fall (13.1 ng m^{-3} on November 23, 2005 at the ZB site and 10.7 ng m^{-3} on November 2, 2005 at the JD) that exceeded the guideline value. Because B*a*P is thought to be easily decomposed in "reactive" air by light and oxidants, the ratio of B*a*PE to B*a*P may include some information on the

ageing of particulate organics. The same seasonal trends were observed for the ratios at both sites: the highest level occurred in winter, whereas the lowest in fall, and the values in summer and spring were almost equivalent. This indicates the different situations of particulate ageing among seasons. The values at the JD site were correspondingly higher than those at the ZB site, and the spatial variation was similar to the observation in Algiers, Italy, although the ratios in Shanghai were lower (Cecinato 1997).

Gas–particle partitioning of PAHs

The distribution of PAHs between the two phases is usually defined using the particle–gas partition coefficient (K_p) according to the following equation (Yamasaki et al. 1982):

$$K_p = \left([F]/[\mathrm{TSP}]/[A]\right) \quad (1)$$

where $[F]$ and $[A]$ are the individual PAH concentrations (nanograms per cubic meter) in particle and gas phases, respectively, and [TSP] is the TSP concentration in atmosphere (micrograms per cubic meter). Useful information about the partitioning can be extracted from the linear regression (slope m_r and intercept b_r) of log K_p versus log P_L^o (subcooled liquid vapor pressure, Pa) of the compound (Eq. 2):

$$\log\ K_p = m_r\ \log\ P_L^o + b_r \quad (2)$$

It has been suggested that the slope m_r should be close to −1 under equilibrium conditions (Pankow 1994). However, many field measurements reported the deviation of m_r from −1, and some reasons were proposed (Pankow and Bidleman 1992; Simcik et al. 1998).

For all the samples in this study, the correlation between log K_P and log P_L^o was checked for each PAH whose concentration was above the detection limit in both phases. The temperature-dependent P_L^o values for all PAHs were calculated according to the empirical relationship by Lei et al. (2002). Strong linear correlations between log K_P and log P_L^o were measured in all samples, with R^2 of 0.87 for the ZB site and 0.86 for the JD (Table 4). The slopes (m_r) were −0.77 and −0.74 for the ZB and JD sites, respectively, indicating PAHs in the urban samples were closer to equilibrium than the suburban ones. This may be caused by the elevated height of the ZB site, which was affected by local emission sources to a larger scale than the JD. The slopes at both sites were found to be shallower in warm season than cold season, and this indicates that not only ambient temperature but also different sources and/or chemical transformation of compounds may affect the gas-to-particle partitioning of PAHs.

Polycyclic aromatic hydrocarbons with various molecular weights have been expected to have different equilibrium rates between the two phases (e.g., Gustafson and Dickhut 1997). Therefore, PAHs with various ring numbers were checked in all samples at both sites, and the compounds with moderate concentrations in both gas and particle phases were selected for the partitioning calculation. Totally, there were 139, 244, and 50 paired data for three-ring PAHs (FLU, PHE, and ANT), four-ring PAHs (FLO, PYR, B*a*A, and CHR), and five-ring PAHs (B*b*F and B*k*F)

Table 4 Seasonal variation of the correlation between log K_p and log P_L^o for Shanghai samples

Sampling site	Season	m_r	b_r	R^2	N	p
ZB	Fall	−0.81	−5.03	0.93	74	<0.0001
	Winter	−0.84	−5.02	0.91	48	<0.0001
	Spring	−0.68	−4.59	0.80	47	<0.0001
	Summer	−0.67	−4.50	0.78	53	<0.0001
	Annual	−0.77	−4.83	0.87	222	<0.0001
JD	Fall	−0.76	−4.84	0.88	70	<0.0001
	Winter	−0.83	−5.00	0.86	37	<0.0001
	Spring	−0.77	−4.92	0.90	64	<0.0001
	Summer	−0.57	−4.35	0.77	50	<0.0001
	Annual	−0.74	−4.78	0.86	221	<0.0001

m_r slope, b_r, intercept, R^2 correlation coefficient, N number of data points, and p level of significance

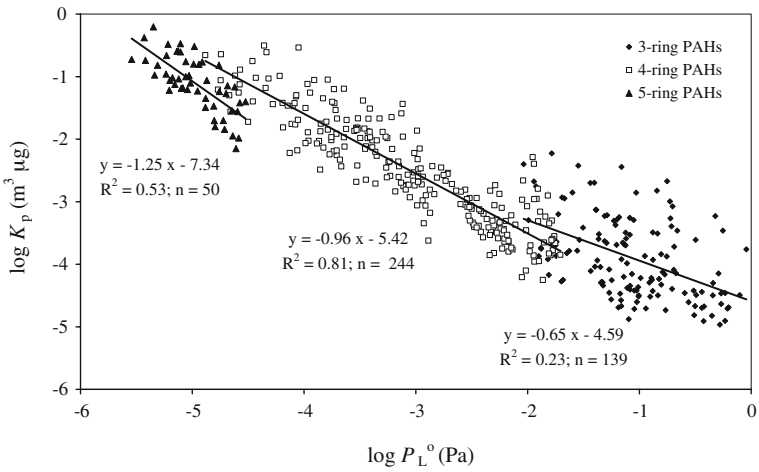

Fig. 3 Correlation between log K_p and log P_L^o for PAH compounds in Shanghai samples

in the calculation, respectively. As Fig. 3 shows, the slope m_r for four-ring PAHs was −0.96, much closer to −1 than for the three-ring (−0.65) and five-ring compounds (−1.25); and a higher correlation coefficient (R^2) was also observed for the four-ring PAHs (0.81) than other groups. Therefore, the four-ring PAHs are suggested to stand for the PAH congeners when their partitioning between gas and particle phases is discussed.

Source apportionment of PAHs

For identification of the major sources of atmospheric PAHs in Shanghai together with the contribution of each source, a multivariate technique, namely, principal component analysis followed by multiple linear regressions (PCA/MLR), was applied to all the samples at both sites. The statistical analysis was performed using SPSS software with the procedure introduced by Thurston and Spengler (1985) and Harrison et al. (1996). Other than the above-discussed 17 compounds, 10 more PAHs were combined into the modeling calculation, including some source markers such as RET and ACP. The total PAH concentrations (gas + particle) were used to eliminate the effects of partitioning between phases (Harrison et al. 1996; Simcik et al. 1999; Larsen and Baker 2003). Values less than the method detection limit (MDL) were substituted by one half of the MDL, and samples with more than 20% of PAHs below MDL were excluded from the matrix (Guo et al. 2003). Finally, 29 and 28 samples were considered for the ZB and JD sites, respectively.

Four principal components were extracted from the data for the two sites separately (Table 5), and their seasonal contributions to total PAH concentration were shown in Fig. 4. At the ZB site, the four factors explained 41.4%, 24.3%, 21.3%, and 4.4%, respectively, with cumulative 91.3% of the total variance. Factor 1 is characterized by high loading of higher-weight PAHs from B*a*A to COR. Some compounds such as B*ghi*P, COR, INP, and B*k*F are indicative of gasoline and diesel engine emissions (Harrison et al. 1996; Larsen and Baker 2003; Venkataraman et al. 1994; Li and Damens 1993; Miguel and Pereira 1989). Therefore, factor 1 is selected to represent vehicular exhaust. This source provides the lowest PAH contribution during summertime (Fig. 4). Factor 2 is highly loaded with FLO, PYR, PHE, and ANT and their methyl derivatives as well as RET and DBT and has a positive correlation ($r = 0.70$, $p < 0.001$) with the ambient temperature. Figure 4 shows the obviously high contribution of this factor in summer samples. Several studies suggested that this factor is linked to ground volatilization process (Dimashki et al. 2001; Li et al. 2006; Wania et al. 1998; Ramdahl 1983), although it is affected by wood smoke to some extent because RET is thought to be a tracer for coniferous wood combustion (Schauer et al. 2001; Ramdahl 1983). Factor 3 is heavily loaded with ACY, DBF, FLU, M-FLU, and ACE. This

factor may be related to coal combustion because ACY and FLU were the dominant PAHs in coke oven and coal burning under different conditions (Masclet et al. 1987; Khalili et al. 1995), and FLU was suggested to represent this source by some studies (Li et al. 2006; Simcik et al. 1999). Figure 4 shows that this source contributed the largest PAH fraction in winter in Shanghai, agreeing with the situation of increasing coal consumption for space heating in this season. Factor 4 is highly loaded with ACP, a good tracer for biomass burning (Shi et al. 2008), and shows small fluctuation in all seasons but fall (Fig. 4), which is in accordance with the commonly happening field combustion after harvest in the nearby rural areas. Yang et al. (2005) also suggested important contribution of biomass burning to the carbonaceous pollution in Shanghai according to the high mass ratios of excessive potassium to elemental carbon.

At the JD site, the four factors were responsible for 38.8%, 25.6%, 17.2%, and 5.7%, respectively, with cumulative 87.3% of the total variance. From Table 5, it can be seen that the profiles of factors 1 to 3 were very similar at the two sites, except factor 2 of the JD site that was combined with high loading of ACP, indicative of the effect

Table 5 Rotated component matrix for total PAHs (gas + particle) in Shanghai

PAHs	ZB site				JD site			
	FC1	FC2	FC3	FC4	FC1	FC2	FC3	FC4
ACY			0.957				0.881	0.254
ACE		0.436	0.683		0.326		0.882	
FLU	0.201	0.263	0.917		0.290		0.903	
M-FLU	0.476	0.275	0.718		0.599		0.687	
DBF		0.271	0.928		0.254		0.924	
PHE	0.355	0.749	0.511			0.881		
ANT	0.338	0.807	0.307	0.205		0.911		
M-PHE	0.311	0.787	0.448			0.919		
FLO		0.891	0.270			0.898		
PYR	0.342	0.860	0.238			0.926		
M-PYR	0.667	0.670	0.235		0.384	0.810		0.365
DBT	0.347	0.822				0.835		
RET		0.957				0.692		0.484
B*a*A	0.921	0.298			0.791	0.409		0.209
CHR	0.821	0.266	0.451		0.896			
M-CHR	0.767	0.259	0.481		0.800		0.437	
B*b*F	0.782		0.535		0.898		0.250	
B*k*F	0.903	0.203	0.301		0.964			
B*e*P	0.917	0.237			0.935		0.216	
B*a*P	0.926	0.273			0.851			
I*cd*P	0.933	0.261			0.957		0.203	
I*cd*F	0.881		0.255		0.739			0.304
B*ghi*F	0.703	0.203	0.611		0.779	0.318	0.369	0.287
B*ghi*P	0.874	0.325			0.777			
DBA	0.932	0.184			0.854		0.245	
COR	0.874	0.207	0.271		0.767		0.293	
ACP				0.952	0.404	0.766	0.243	
% variance	41.38	24.33	21.31	4.40	38.78	25.62	17.20	5.69
% cumulative	41.38	65.71	87.01	91.41	38.78	64.40	81.60	87.29
Source	Vehicle	Volatilization	Coal	Biomass	Vehicle	Volatilization/ biomass	Coal	Unknown

Extraction method: PCA. Rotation method: varimax with Kaiser normalization. Only factor loading values > 0.20 are presented

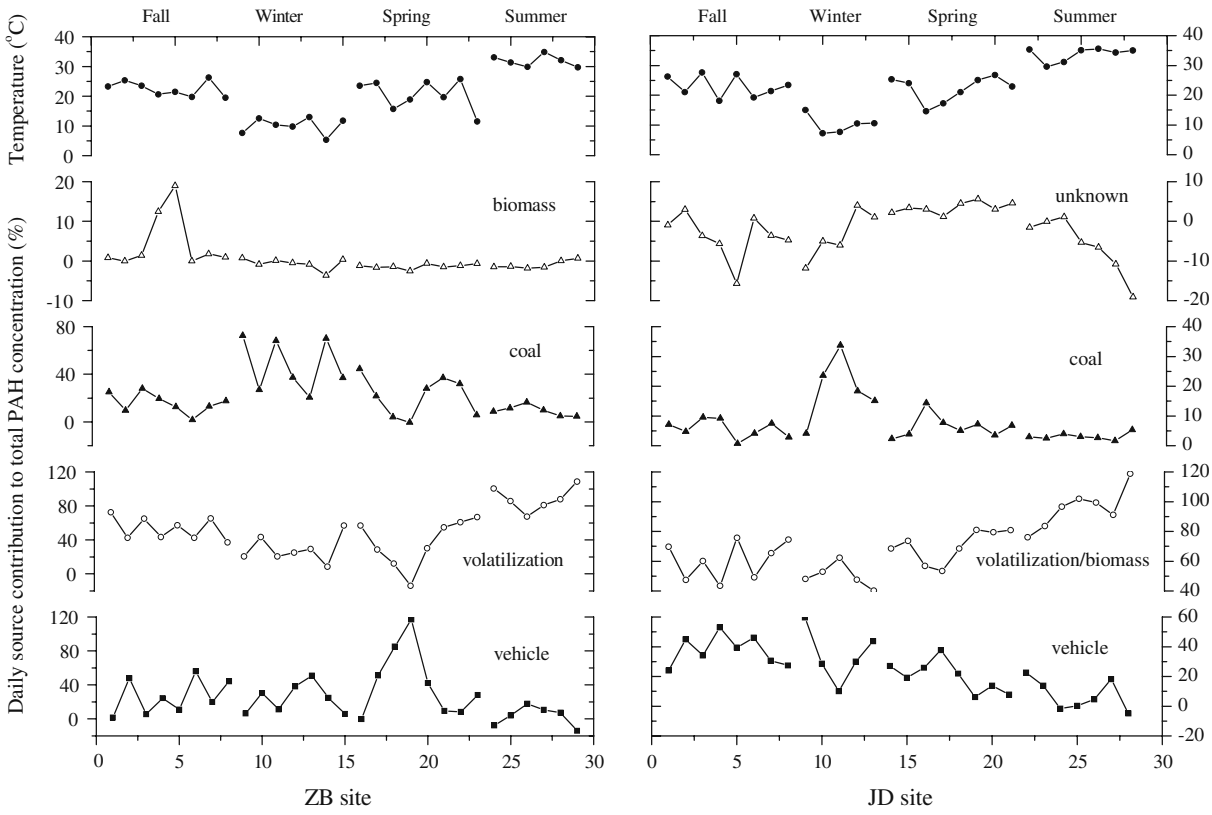

Fig. 4 Time series of daily source contribution to total PAH concentrations in Shanghai

by biomass burning. Factor 4 is an unidentified source, with no significant loading of any PAHs. This factor shows positive contribution only in spring (Fig. 4) and might be related to the road dust. However, more information such as inorganic data is needed for this inference.

According to the results of the MLR analysis, the annual contribution of each identified source to the total PAH mass was calculated. At the urban site, the four sources (vehicle, volatilization, coal, and biomass) accounted for 25.4 ± 28.4%, 50.3 ± 28.5%, 23.8 ± 20.0%, and 0.5 ± 4.5%, respectively, while at the suburban site, the four sources (vehicle, volatilization/biomass, coal, and unknown source) emitted 24.4 ± 16.7%, 70.2 ± 19.7%, 7.6 ± 7.4%, and −2.2 ± 6.3%, respectively. That is to say, evaporation from contaminated ground was the most important source of atmospheric PAHs in Shanghai. Li et al. (2006) also reported that this source contributed 68% of PAHs in Guangzhou. Vehicles and coal emitted the other fraction (32.0–49.2%) in Shanghai and should be controlled when atmospheric PAHs were concerned.

Conclusions

In this study, PAH compounds were quantified in ambient samples collected at urban and suburban sites in Shanghai during four seasonally representative months during 2005–2006, with their seasonal variations, and gas–particle partitioning and potential sources were characterized. The results showed that the total concentrations (gas + particle) of 17 PAHs were 167–216 ng m^{-3} at the two sites, and PHE, FLO, PYR, ANT, and FLU were among the dominant compounds. The particulate PAHs constituted less than 30% of total concentration but contributed more than 90%

of total toxic power of PAHs. Different seasonal trends of PAH concentrations were observed at the two sites, which may be attributable to complicated factors such as sampling heights, local–regional emission sources, and climatic conditions. Strong linear correlations between log K_p and log P_L^o were measured in all samples, with shallower slopes m_r observed at the suburban site than the urban site and in warm season than in a cold month, indicating the different equilibrium conditions of PAHs in spatial and temporal scales in Shanghai. Based on the PCA/MLR, the potential sources of atmospheric PAHs were estimated. Vehicles and coal consumption were the two important PAH emission sources other than volatilization, which totally contributed about one third (suburban area) to one half (urban area) of PAH mass in Shanghai atmosphere.

Acknowledgements This work was supported by the National Natural Science Foundations of China (40605033, 40773047, and 40973071), Knowledge Innovative Programs of CAS (KZCX2-YW-Q07-04, KZCX2-YW-QN210, and KZCX1-YW-06), and the Department of Science and Technology of Shandong Province (2007GG2QT06018). We would like to thank for the assistance about sampling from the Environmental Monitoring Station of Jia-ding District in Shanghai. We would also thank the anonymous reviewers for their help in revisions.

References

Bi, X., Sheng, G., Peng, P., Chen, Y., Zhang, Z., & Fu, J. (2003). Distribution of particulate- and vapor-phase *n*-alkanes and polycyclic aromatic hydrocarbons in urban atmosphere of Guangzhou, China. *Atmospheric Environment, 37*, 289–298.

Bidleman, T. F. (1988). Atmospheric processes: Wet and dry deposition of organic compounds are controlled by their vapor-particle partitioning. *Environmental Science & Technology, 22*, 361–367.

Bozlaker, A., Muezzinoglu, A., & Odabasi, M. (2008). Atmospheric concentrations, dry deposition and air–soil exchange of polycyclic aromatic hydrocarbons (PAHs) in an industrial region in Turkey. *Journal of Hazardous Materials, 153*, 1093–1102.

Cecinato, A. (1997). Polynuclear aromatic hydrocarbons (PAH), benz(*a*)pyrene (B*a*PY) and nitrated-PAH (NPAH) in suspended particulate matter. *Annali di Chimica, 87*, 483–496.

Chen, G. (2003). Orientation of the types of Shanghai air pollution. *Shanghai Environmental Science, 22*, 230–233 (in Chinese).

Chen, Y., Sheng, G., Bi, X., Feng, Y., Mai, B., & Fu, J. (2005). Emission factors for carbonaceous particles and polycyclic aromatic hydrocarbons from residential coal combustion in China. *Environmental Science & Technology, 39*, 1861–1867.

Cincinelli, A., Bubba, M. D., Martellini, T., Gambaro, A., & Lepri, L. (2007). Gas–particle concentration and distribution of n-alkanes and polycyclic aromatic hydrocarbons in the atmosphere of Prato (Italy). *Chemosphere, 68*, 472–478.

Dachs, J., Glenn, T. R., IV, Gigliotti, C. L., Brunciak, P., Totten, L. A., Nelson, E. D. et al. (2002). Processes driving the short-term variability of PAHs in the Baltimore and northern Chesapeake Bay atmosphere, USA. *Atmospheric Environment, 36*, 2281–2295.

Dimashki, M., Lim, L. H., Harrison, R. M., & Harrad, S. (2001). Temporal trends, temperature dependence, and relative reactivity of atmospheric polycyclic aromatic hydrocarbons. *Environmental Science & Technology, 35*, 2264–2267.

Fang, G. C., Chang, K. F., Lu, C., & Bai, H. (2004). Estimation of PAHs dry deposition and B*a*P toxic equivalency factors (TEFs) study at Urban, Industry Park and rural sampling sites in central Taiwan, Taichung. *Chemosphere, 55*, 787–796.

Feng, Y., Chen, Y., Guo, H., Zhi, G., Xiong, S., Li, J., et al. (2009). Characteristics of organic and elemental carbon in $PM_{2.5}$ samples in Shanghai, China. *Atmospheric Research, 92*, 434–442.

Finlayson-Pitts, B. J., & Pitts, J. N., Jr. (2000). *Chemistry of the upper and lower atmosphere*. San Diego, CA: Academic Press.

Guo, H., Lee, S. C., Ho, K. F., Wang, X. M., & Zou, S. C. (2003). Particle-associated polycyclic aromatic hydrocarbons in urban air of Hong Kong. *Atmospheric Environment, 37*, 5307–5317.

Gustafson, K. E., & Dickhut, R. M. (1997). Particle/gas concentrations and distributions of PAHs in the atmosphere of southern Cheaspeake Bay. *Environmental Science & Technology, 31*, 140–147.

Harrison, R. M., Smith, D. J. T., & Luhana, L. (1996). Source apportionment of atmospheric polycyclic aromatic hydrocarbons collected from an urban location in Birmingham, UK. *Environmental Science & Technology, 30*, 825–832.

IARC (1987). *IARC monographs on the evaluation of carcinogenic risks to humans: An updating of IARC monographs* (Vols. 1–42, Supplement 7). Lyon, France.

Khalili, N. R., Scheff, P. A., & Holsen, T. M. (1995). PAH source fingerprints for coke ovens, diesel and gasoline engines, highway tunnels, and wood combustion emissions. *Atmospheric Environment, 29*, 533–542.

Larsen, R. K., & Baker, J. E. (2003). Source apportionment of polycyclic aromatic hydrocarbons in the urban atmosphere: A comparison of three methods. *Environmental Science & Technology, 37*, 1873–1881.

Lei, Y. D., Chankalal, R., Chan, A., & Wania, F. (2002). Supercooled liquid vapor pressures of the polycyclic aromatic hydrocarbons. *Journal of Chemical & Engineering Data, 47*, 801–806.

Li, C. K., & Damens, R. M. (1993). The use of polycyclic aromatic hydrocarbons as source signatures in receptor modeling. *Atmospheric Environment, 27A*, 523–532.

Li, J., Zhang, G., Li, X. D., Qi, S. H., Liu, G. Q., & Peng, X. Z. (2006). Source seasonality of polycyclic aromatic hydrocarbons (PAHs) in a subtropical city, Guangzhou, South China. *Science of the Total Environment, 355*, 145–155.

Liu, M., Cheng, S. B., Ou, D. N., Hou, L. J., Gao, L., Wang, L. L., et al. (2007). Characterization, identification of road dust PAHs in central Shanghai areas, China. *Atmospheric Environment, 41*, 8785–8795.

Mandalakis, M., Tsapakis, M., Tsoga, A., & Stephanou, E. G. (2002). Gas–particle concentrations and distribution of aliphatic hydrocarbons, PAHs, PCBs and PCDD/Fs in the atmosphere of Athens (Greece). *Atmospheric Environment, 36*, 4023–4035.

Masclet, P., Bresson, M. A., & Mouvier, G. (1987). Polycyclic aromatic hydrocarbons emitted by power stations, and influence of combustion conditions. *Fuel, 66*, 556–562.

Miguel, A., & Pereira, P. (1989). Benzo(*k*)fluoranthene, benzo(*ghi*)perylene, and indeno(1,2,3-*cd*)pyrene: New tracers of automotive emissions in receptor modeling. *Aerosol Science & Technology, 10*, 292–295.

Odabasi, M., Vardar, N., Sofuoglu, A., Tasdemir, Y., & Holsen, T. M. (1999). Polycyclic aromatic hydrocarbons (PAHs) in Chicago air. *Science of the Total Environment, 227*, 57–67.

Offenberg, J. H., & Baker, J. E. (2002). The influence of aerosol size and organic carbon content on gas/particle partitioning of polycyclic aromatic hydrocarbons (PAHs). *Atmospheric Environment, 36*, 1205–1220.

Ohura, T., Amagai, T., Fusaya, M., & Matsushita, H. (2004). Spatial distributions and profiles of atmospheric polycyclic aromatic hydrocarbons in two industrial cities in Japan. *Environmental Science & Technology, 38*, 49–55.

Pankow, J. F. (1994). An absorption model of gas/particle partitioning of organic compounds in the atmosphere. *Atmospheric Environment, 28*, 185–188.

Pankow, J. F., & Bidleman, T. F. (1992). Interdependence of the slopes and intercepts from log-log correlations of measured gas–particle partitioning and vapor pressure. I. Theory and analysis of available data. *Atmospheric Environment, 26A*, 1071–1080.

Park, S. S., Kim, Y. J., & Kang, C. H. (2002). Atmospheric polycyclic aromatic hydrocarbons in Seoul, Korea. *Atmospheric Environment, 36*, 2917–2924.

Poor, N., Tremblay, R., Kay, H., Bhethanabotla, V., Swartz, E., Luther, M., et al. (2004). Atmospheric concentrations and dry deposition rates of polycyclic aromatic hydrocarbons (PAHs) for Tampa Bay, Florida, USA. *Atmospheric Environment, 38*, 6005–6015.

Possanzini, M., Di Palo, V., Gigliucci, P., Sciano, M. C. T., & Cecinato, A. (2004). Determination of phase-distribution PAH in Rome ambient air by denuder/GC-MS method. *Atmospheric Environment, 38*, 1727–1734.

Ramdahl, T. (1983). Retene—A molecular marker of wood combustion in ambient air. *Nature, 306*, 580–582.

Ravindra, K., Sokhi, R., & Grieken, R. V. (2008). Atmospheric polycyclic aromatic hydrocarbons: Source attribution, emission factors and regulation. *Atmospheric Environment, 42*, 2895–2921.

Schauer, J. J., Kleeman, M. J., Cass, G. R., & Simoneit, B. R. T. (2001). Measurement of emissions from air pollution sources. 3. C1-C29 organic compounds from fireplace combustion of wood. *Environmental Science & Technology, 35*, 1716–1728.

Shi, Q., Wang, T. G., Zhong, N. N., Zhang, Z. H., & Zhang, Y. H. (2008). Identification of acephenanthrylene and aceanthrylene in aerosol and its environmental implication. *Chinese Science Bulletin, 53*, 890–894.

Simcik, M. F., Eisenreich, S. J., & Lioy, P. J. (1999). Source apportionment and source/sink relationships of PAHs in the coastal atmosphere of Chicago and Lake Michigan. *Atmospheric Environment, 33*, 5071–5079.

Simcik, M. F., Franz, T. P., Zhang, H., & Eisenreich, S. (1998). Gas-particle partitioning of PCBs and PAHs in the Chicago urban and adjacent coastal atmosphere: States of equilibrium. *Environmental Science & Technology, 32*, 251–257.

Thurston, G. D., & Spengler, J. D. (1985). A quantitative assessment of source contributions to inhalable particulate matter pollution in metropolitan Boston. *Atmospheric Environment, 19*, 9–25.

Tsapakis, M., & Stephanou, E. G. (2005). Occurrence of gaseous and particulate polycyclic aromatic hydrocarbons in the urban atmosphere: Study of sources and ambient temperature effect on the gas/particle concentration and distribution. *Environmental Pollution, 133*, 147–156.

Vasilakos, Ch., Levi, N., Maggos, Th., Hatzianestis, H., Michopoulos, J., & Helmis, C. (2007). Gas-particle concentration and characterization of sources of PAHs in the atmosphere of a suburban area in Athens, Greece. *Journal of Hazardous Materials, 140*, 45–51.

Venkataraman, C., Lyons, J. M., & Friedlander, S. K. (1994). Size distributions of polycyclic aromatic hydrocarbons and elemental carbon. 1. Sampling, measurement methods, and source characterization. *Environmental Science & Technology, 28*, 555–562.

Wania, F., Haugen, J. E., Lei, Y. D., & Mackay, D. (1998). Temperature dependence of atmospheric concentrations of semivolatile organic compounds. *Environmental Science & Technology, 32*, 1013–1021.

Yamasaki, H., Kuwata, K., & Miyamoto, H. (1982). Effects of ambient temperature on aspects of airborne polycyclic aromatic hydrocarbons. *Environmental Science & Technology, 16*, 189–194.

Yang, F., He, K., Ye, B., Chen, X., Cha, L., Cadle, S. H., et al. (2005). One-year record of organic and elemental carbon in fine particles in downtown Beijing and Shanghai. *Atmospheric Chemistry & Physics, 5*, 1449–1457.